UNIVERSITY OF OKLAHOMA

GRADUATE COLLEGE

NOVEL TARGETED ANNEXIN V–NANOPARTICLE CONJUGATE FOR CANCER PHOTOPHERMAL THERAPY

A THESIS

SUBMITTED TO THE GRADUATE FACULTY

in partial fulfillment of the requirements for the

Degree of

Master of Science

By

CLEMENT GUILLAUME KARCH

Norman, Oklahoma

2020

NOVEL TARGETED ANNEXIN V–NANOPARTICLE CONJUGATE
FOR CANCER PHOTOPHERMAL THERAPY

A THESIS APPROVED FOR THE
STEPHENSON SCHOOL OF BIOMEDICAL ENGINEERING

BY THE COMMITTEE CONSISTING OF

Dr. Roger Harrison, Chair

Dr. Lacey McNally

Dr. Robert Shambaugh

Acknowledgements

I thank the members of my committee, Dr. Lacey McNally, Dr. Robert Shambaugh, and Dr. Roger Harrison, for all the help they were able to give me during this research project.

I would particularly like to thank my mentor, Dr Roger Harrison, for allowing me to work in his laboratory, for sharing his knowledge with me and for his guidance throughout this research project. I also wish to thank Polytech Clermont-Ferrand, and especially Dr. Jane Roche, Dr. Cédric Delattre, Dr. Sébastien Lageix and Dr. Guillaume Pierre, without whom this dual degree at the University of Oklahoma would not have been possible.

I would also like to thank the members and interns of Dr. Harrison's laboratory, Gabriela Nogueira Furtado E Faria, Alexis Woodward, Adam Aissanou and Anitha Abitugenera with whom I had the pleasure and the opportunity to work with. I also want to thank Amy Burke and Sandra Doan for their training, their knowledge, and their time. I also want to thank my family and friends for the moral support they gave me.

This research experience was outstanding for me and allowed me to evolve in a very dynamic international environment. All this could not have happened without your help. Thank you.

Table of contents

List of figures:

List of abbreviations:

Anx V: annexin V

CD: cluster differentiation

CTLA-4: cytotoxic T-lymphocyte-associated protein 4

DSPE-PEG-MAL linker: 1,2-distearoyl-sn-glycero-3-phosphoethanolamine-N maleimide(polyethylene glycol) linker

EDTA: ethylenediaminetetraacetic acid

FBS: fetal bovine serum

HER2: human epidermal growth factor receptor 2

IFNγ: interferon gamma

IL-6: Interleukin 6

IL-12 (p70): Interleukin 12

IPTG: isopropyl β-D-1-thiogalactopyranoside

IT: intratumoral

IV: intravenous

MWCNT: multi-walled carbon nanotubes

PMSF: phenylmethylsulfonyl fluoride

PS: phosphatidylserine

PTT: photothermal therapy

SWCNT: single-walled carbon nanotube

TNBC: triple negative breast cancer

TNFα: tumor necrosis factor

TPCK: tosyl phenylalanyl chloromethyl ketone

Abstract

Triple negative breast cancer represents a strong clinical challenge due to its high invasiveness and the lack of therapeutic targets. To overcome this problem, recent combination therapeutic strategies have been implemented. When treated during early phases, a combination of surgery, chemotherapy, and irradiation therapy is usually performed, which significantly improves the overall survival of the patients. However, when detected later, triple negative breast cancer begins to metastasize, considerably reducing the effectiveness of the treatments. As a potential solution to this problem, we propose a novel treatment of metastatic triple negative breast cancer that combines targeted photothermal therapy with a checkpoint inhibitor treatment. Photothermal therapy is a recent irradiation therapy based on the electromagnetic radiation of photosensitizers. When exposed to specific electromagnetic radiation, photosensitizers absorb irradiating energy and releases it as heat to the surrounding environment. The resulting heat can be used to disrupt the membranes of cancer cells or to denature essential cytoplasmic proteins, inducing tumor elimination. This approach is interesting because it can induce the release of tumor antigens and proinflammatory cytokines that can be used to treat metastases.

The effectiveness of a novel targeted conjugate for targeted photothermal therapy based on single-walled carbon nanoparticles was assessed *in vitro*, and the ability of the treatment to release proinflammatory cytokines in mice was demonstrated. This new treatment showed significant cytotoxicity against EMT6 triple negative breast cancer cells, while not affecting the cell viability of a healthy endothelial cell model *in vitro*. In a mouse model, the treatment has shown to be effective in releasing cytokines TNFα, IFNγ and IL-6 into the bloodstream of the mice. By combination with the checkpoint inhibitor anti-CTLA-4, this approach has shown promising results in the treatment of triple negative breast cancer metastases in mice.

Chapter 1: Introduction

1.1. Cancer and treatment strategies

Cancer is a broad group of pathologies occurring in a large number of animal species[1-5]. Cancer can be described as an abnormal cell growth, starting in an organ and gradually invaded by the tumor cells. At advanced stages, cancer can potentially spread to other parts of the body [6-8]. Briefly, cancer stages can be separated in five categories. The first one is Stage 0; at this stage the tumor is still located at the initial abnormal division site, and cancer does not start to spread to surrounding tissues [9]. At Stage I, also called early-stage cancer, tumor cells will start to invade nearby tissues [9]. The tumor size is still small (generally less than 2 cm), and the cancer cells have not spread yet to the neighboring lymph nodes. Stage II and Stage III cancers correspond to larger tumors (generally 2 cm to 5 cm for Stage II, and more than 5 cm for stage III), and lymph nodes may be invaded by cancer cells at these stages [9]. Stage IV, also called metastatic or advanced stage, corresponds to large tumor spreading to other organs and body parts [9].

1.1.1. Triple negative breast cancer

Triple negative breast cancer (TNBC) is a highly aggressive sub-type of breast cancer, and it has been reported to occur in 15% to 20% of the total breast cancer cases [10]. Triple negative breast cancers do not express the progesterone receptor, estrogen receptor or HER-2 genes [11]. These receptors are usually used to target breast cancer and to treat them via endocrine therapy [12]. For this reason, endocrine therapy is ineffective on TNBC, and TNBC currently represent a strong clinical challenge due to the lack of

existing efficient targeted treatments [12]. This lack of receptors also makes the development of new targeted therapies more difficult. TNBC tumors are highly invasive and metastatic. They present a poorer prognosis over a period of 5 years post-diagnosis when compared to estrogen-positive breast cancers [13-15].

1.1.2. Current treatments for triple negative breast cancer

Triple negative breast cancer is generally detected and diagnosed at stage II or early III, leaving the opportunity of resorting to surgery or radiation therapy as a treatment [16-18]. Patients with TNBC are usually treated with a combination of surgery and chemotherapy[19] . Among the chemotherapies that can be used to treat TNBC there are:

- Anthracyclines (such as doxorubicin or idarubicin). These molecules intercalate in the DNA of tumor cells and induce a local change in the structure of the DNA strand, thereby inhibiting replication processes. Furthermore, anthracyclines are inhibitors of type II DNA topoisomerases, enzymes involved in the DNA replication and transcription [20].
- The alkylating agents (such as cyclophosphamide or chlormethine). These molecules interact with the purines of the DNA and add alkyl groups to them. Cancer cells have a very rapid metabolism. Their proliferation is faster than healthy cells, and the mechanisms for controlling and correcting DNA replication errors are altered. For these reasons, cancer cells are more susceptible to DNA damage, including alkylation[21].
- The taxanes (such as paclitaxel or docetaxel). These molecules target β tubulin and disrupt the function of the microtubules. β tubulin are responsible for the

spindle apparatus and chromosome migration during cell migration. By inhibiting β tubulin, the taxanes inhibit cancer cells division[22].

In addition to chemotherapy, TNBC patients are also treated with surgery and radiation therapy [19]. Patients treated with radiation therapy in addition to chemotherapy and surgery shows a lower risk of new tumor development on a treated site (locoregional recurrence), and an improved overall survival [23-25]. Radiation therapy is a key asset in combinatorial treatments of triple negative breast cancer, and a promising field to be explored to improve current TNBC treatments. However, when cancer is detected at later stages, metastases may start to develop, making irradiation therapy less effective. In this thesis, we explore the use of a recent form of irradiation therapy, photothermal therapy, which could be used in the treatment of TNBC metastases.

1.2. Photothermal therapy

1.2.1. Principles of photothermal therapy

Photothermal therapy (PTT) is a form of radiation therapy using electromagnetic radiation. Molecules able to absorb electromagnetic radiation, called photosensitizers, can be irradiated by a photon beam, and enter transition to an excited state [26]. The energy accumulated by the photosensitizers is then released to the nearby environment in the form of heat [26]. Nanoparticles are commonly used as photosensitizers, and nanoparticles such as carbon nanotubes [27,28], gold nanorods [29,30] or silica-based nanoparticles [31,32] have for example been tested for photothermal therapy in the treatment of cancer. The heat generated during PTT is due to vibrations of the nanoparticle on a molecular level after being exposed to electromagnetic radiation [33]. It has been shown that the heat

resulting from PTT is sufficient to eliminate cancer cells via necrosis by rupture of the cell membranes, or via hyperthermia by denaturation of cytoplasmic proteins [34,35]. Necrosis occurs at temperature above 47°C[36,37].

1.2.2. Carbon nanotubes

Carbon nanotubes are tubes composed only of carbon atoms with a diameter of a few nanometers. Carbon nanotubes can be classified into two categories: single-walled carbon nanotubes (SWCNTs) and multi-walled carbon nanotubes (MWCNTs) [38]. Although they are not synthesized like that, we can represent the SWNTs as a series of carbon hexagons coiled to form a tube. The MWCNTs correspond to SWCNTs nested within each other and linked together by weak bounds [39]. A representation is shown in **Figure 1.**

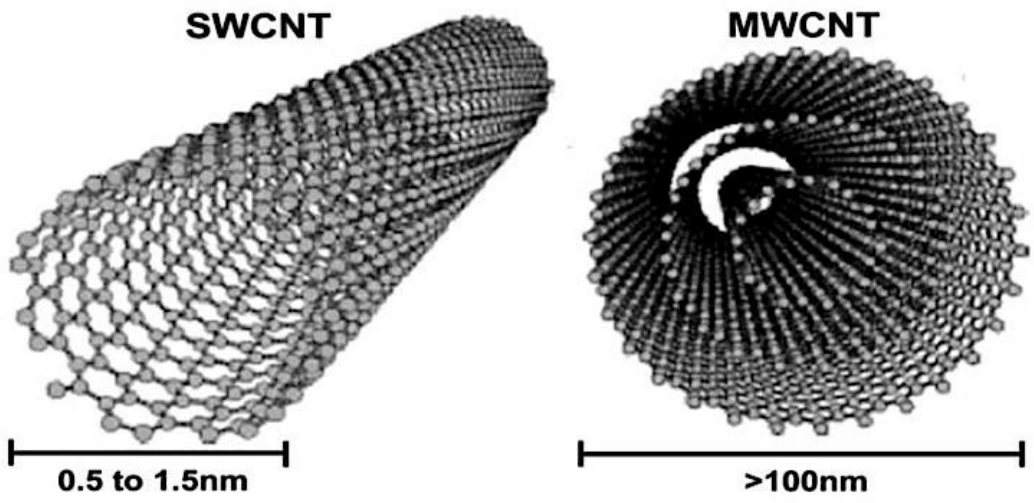

Figure 1: Single-walled and multi-walled carbon nanotubes representation [40]. Single walled carbon nanotubes are represented on the left, and multi-walled carbon nanotubes appears as nested SWNTs on the right.

SWCNTs present a high stability and are much less toxic to cells than MWCNTs [41-43]; for these reasons SWCNTs are used for photothermal therapy over MWCNTs in this

study. Moreover, the average external diameter of SWCNTs is shorter than the diameter of MWCNTs, facilitating its transport in the bloodstream for potential *in vivo* studies.

1.3. Carbon nanotube conjugation for a targeted photothermal therapy

Nanotube carbons being inert, they must be conjugated to a targeting agent in order to be able to carry out targeted photothermal therapy.

1.3.1. Phosphatidylserine and triple negative breast cancer targeting

Phosphatidylserine is phospholipid involved in the apoptosis pathway and that can be used to detect apoptotic cells in an injured tissue [44,45]. In healthy cells, phosphatidylserines are found in the inner layer of the cell membrane [46]. Phosphatidylserine (PS) is externalized on the outer layer of the plasma membrane and serves notably as a signal for cell death in apoptotic cells [47]. Most cancer cells have been shown to express the PS on the outer layer of their cell membrane [48]. This mechanism is used by cancer cells to trick the immune system into masquerading as apoptotic cells. This PS externalization is also found in TNBC and can be used as a target for targeted photothermal therapy [49].

1.3.2. Annexin V and targeted photothermal therapy

Annexin V (anx V) is a protein whose complete functions are still unknown today. However, this protein is commonly used in flow cytometry for its properties to label apoptotic cells [44,45].

It has been shown that anx V is capable of fixing the PS externalized by apoptotic cells[43,44]. Likewise, annexin V can be used to bind the PS externalized by cancer cells. Human annexin V is composed of 320 amino acids. The complete sequence is shown in **Figure 2:**

MAQVLRGTVTDFPGFDERADAETLRKAMKGLGTDEESILTLLTSRSNAQRQE
ISAAFKTLFGRDLLDDLKSELTGKFEKLIVALMKPSRLYDAYELKHALKGAG
TNEKVLTEIIASRTPEELRAIKQVYEEEYGSSLEDDVVGDTSGYYQRMLVVLL
QANRDPDAGIDEAQVEQDAQALFQAGELKWGTDEEKFITIFGTRSVSHLRKV
FDKYMTISGFQIEETIDRETSGNLEQLLLAVVKSIRSIPAYLAETLYYAMKGAG
TDDHTLIRVMVSRSEIDLFNIRKEFRKNFATSLYSMIKGDTSGDYKKALLLL**C**
GEDD

Figure 2: Human annexin V amino acids sequence [49]. This image shows the amino acids sequence of human annexin V, each letter corresponding to an amino acid. The sequence has a cysteine (boxed in yellow) in position 316.

Annexin has in its sequence a cysteine whose sulfhydryl group will be used for its conjugation. The approach used in this thesis consists in conjugating SWNCTs with annexin V in order to create a photosensitizer targeted to triple negative breast cancer cells. The conjugate will bind to the PS externalized by cancer cells thanks to annexin V. The conjugation between carbon nanotubes and annexin V will be done through a linker: the1,2-distearoyl-sn-glycero-3-phospho ethanolamine-N-maleimide (polyethylene glycol), also called DSPE-PEG-MAL linker (shown in **Figure 3**):

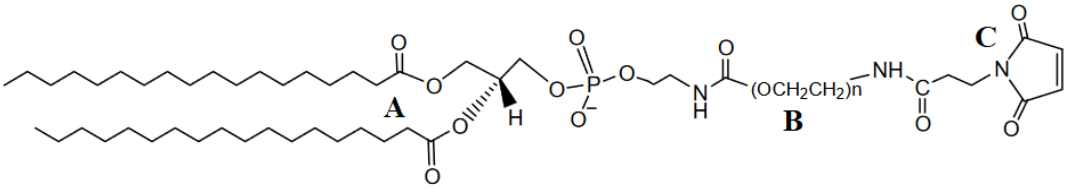

Figure 3: Structural formula of the 1,2-distearoyl-sn-glycero-3-phospho ethanolamine-N-maleimide(polyethylene glycol) linker [50]. The structure contains two aliphatic tail (A), a polyethylene glycol molecule (B), and a maleimide molecule (C).

The DSPE-PEG-MAL linker has in its structure a maleimide molecule which can react with the sulfhydryl groups of cysteines to form a thioether. This property will be used later to conjugate annexin V to the linker. SWCNTs are only composed of carbon atoms and are therefore very hydrophobic. The linker has long hydrophobic aliphatic tails capable of attaching to nanotube carbons. In addition to the targeted aspect, the conjugation between SWCNTs and Annexin V improves the solubility of nanotubes. The DSPE-PEG-MAL linker also has a polyethylene glycol molecule in its structure which reduces the immunogenicity and antigenicity of the conjugate.

1.3.3. Combining checkpoint inhibitors and photothermal therapy

Upon exposure to a pathogen, an initial immune response occurs: the cell-mediated immunity. This immune response involves the activation of phagocytes capable of eliminating pathogens by phagocytosis mechanisms. This immune response also involves the activity of T lymphocytes, which can be classified into different categories:

- Cytotoxic CD8+ T cells: Once activated by contact with class I MHC-antigen complexes, these cells release perforin onto the pathogen. Perforin is a protein

capable of inserting into the membrane of targeted pathogens to form holes. The pathogen's membrane is disrupted, and the pathogen is eliminated.

- Helper CD4+ T cells: These cells are activated by antigen presenting cells. The main functions of the Helper CD4+ T cells are the activation of cytotoxic T cells and macrophages, as well as the release of proinflammatory cytokines. One of the main cytokines released is interferon gamma (IFNγ), which activates macrophages. Interferon gamma is also produced by the cytotoxic T cells.
- Regulatory CD4+ T cells: In adults, T lymphocytes are produced in the bone marrow and matured in the thymus where they undergo selection to avoid autoimmune phenomena. The role of the regulatory T cells is to eliminate autoimmune T cells that have escaped selection in the thymus, and to regulate the cell-mediated immune response.

After a first encounter with a pathogen, a second immunity occurs: the humoral immunity. In brief, this immunity is characterized by the production of antibodies by B lymphocytes. The B lymphocytes are able to internalize antigens and to present them on the surface of their membrane via their class II MHC. The complex class II MHC-antigen binds to the helper CD4+ T cells, inducing B lymphocyte proliferation. During a future encounter with the same antigen, these B lymphocytes cells produce a large number of antibodies targeting this antigen. Immune response mechanisms are regulated by immune checkpoints whose role is to prevent autoimmune responses. However, these immune checkpoints can be exploited by cancer cells to avoid being eliminated by the immune system. One of these checkpoints is the protein receptor CTLA-4 or cytotoxic T-lymphocyte-associated protein 4. The ligands for CTLA-4 are the cluster differentiation (CD) 80 and 86, present on the surface of antigen presenting cells. Regulatory CD4+ T

cells constitutively express CTLA-4 on their surface, and a CTLA-4 binding to CD80 or CD86 induces the lymphocyte inactivation. This mechanism is abused by cancer cells which induce the expression of CTLA-4 on the surface of other types of T lymphocytes in order to inhibit their activity. To overcome this problem, an antibody targeting CTLA4 (anti-CTLA-4) can be used. Anti-CTLA-4 binds to CTLA4 and prevents its interaction with CD80 or CD86. Our approach is to combine anti-CTLA-4 with photothermal therapy, as illustrated in **Figure 4**:

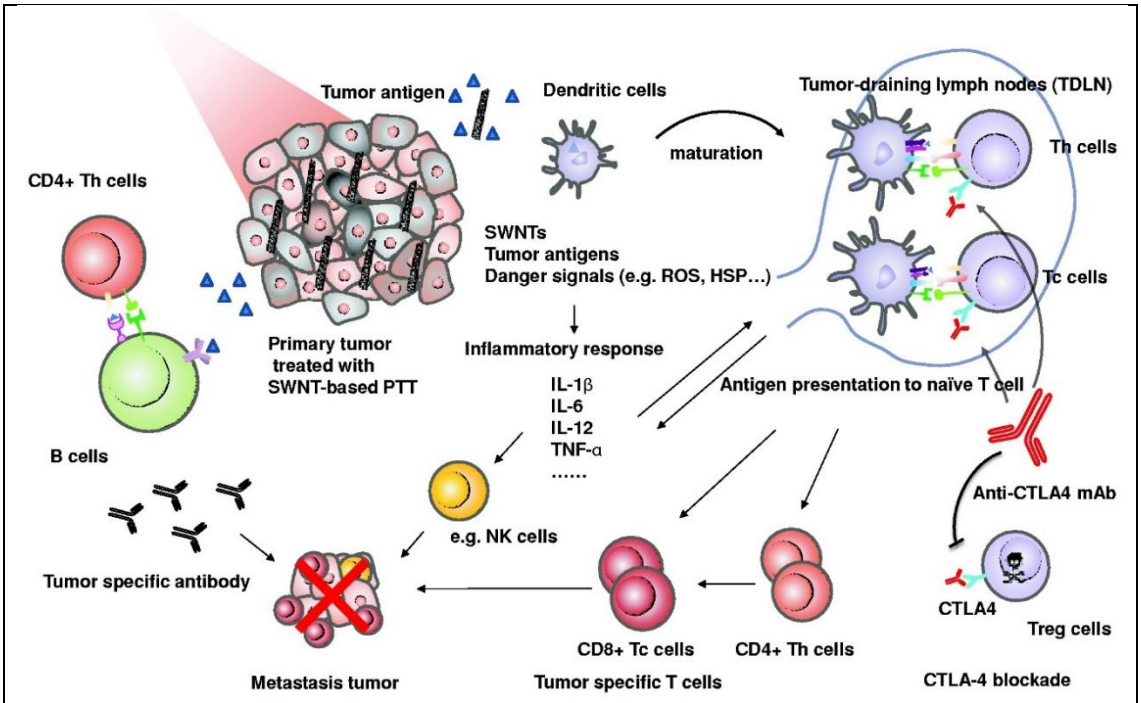

Figure 4: Mechanisms of anti-tumor immune response induced by anti-CTLA-4 treatment combined to photothermal therapy [51]. Photothermal therapy eliminate the primary tumor and induces the release of tumor antigens which are internalized by antigen presenting cells. Anti-CTLA 4 blocks the CTLA-4 of the regulatory T cells and prevents the regulation of the immune response. The antigen presenting cells then activate the cytotoxic and helper T cells, inducing a cell-mediated immune response against the metastases. The helper T cells activate B lymphocytes proliferation, and antibodies targeting the tumor antigens are produced.

Photothermal therapy of a primary tumor induces the release of tumor antigens which can induce an immune response. Anti-CTLA-4 helps prevent the immune response from being regulated. The induced immune response participates in the elimination of other tumors distant from the irradiation site, this mechanism is called the abscopal effect.

1.4. Scope of Study

Hypothesis:

An SWCNT-anx V conjugate for PTT can specifically target cancer cells and be activated via near infrared lights to induce a photothermal effect. The heat generated by the conjugate is sufficient to induce a cell death and can be used to treat triple negative breast cancer models *in vitro* and *in vivo.*

Aim 1: Photothermal therapy studies on a triple negative breast cancer model in vitro:

The objectives are **(1)** to treat EMT6 cells with the SWCNT-anx V conjugate combined with laser irradiation and measure the tumor temperature elevation and cytotoxicity post treatment at room temperature, **(2)** to treat EMT6 cells at 37°C, to assess the post treatment cytotoxicity, and verify the specificity of the conjugate using non-targeted SWCNTs as a control, and **(3)** to assess the effect of treatment on the viability of healthy endothelial HUVEC cells.

Aim 2: Photothermal therapy studies on a triple negative breast cancer model in vivo:

The objectives are **(1)** to compare intravenous and intratumoral injections of SWCNT-anx V combined with photothermal therapy for their ability to release proinflammatory

cytokines, **(2)** to determine the release of proinflammatory cytokines as a function of time in mice at various tumor temperatures, and **(3)** to combine SWCNT-anx V photothermal therapy with anti-CTLA-4 treatment and to quantify the release of proinflammatory cytokines into the bloodstream of the mice.

Chapter 2: Materials and Method

2.1. Materials

pET-30 Ek/LIC plasmid was constructed and sequenced by EMD Chemicals (Billerica, MA). Alamar Blue reagent, isopropyl β-D-1-thiogalactopyranoside (IPTG), tosyl phenylalanyl chloromethyl ketone (TPCK), phenylmethylsulfonyl fluoride (PMSF), ethylenediaminetetraacetic acid (EDTA) were purchased from Sigma-Aldrich (St Louis, MO). HRV-C3 protease was purchased from Sino Biologics (Portland, OR). Dialysis membranes (2kDA, 14kDa and 100kDa) were purchased from Spectrum Laboratories (Rancho Dominguez, CA). Murine triple negative breast cancer cells EMT6 (ATCC® CRL-2755™), human umbilical vein endothelial cells HUVEC (ATCC® CRL-1730™), Waymouth's MB 752/1 medium, and vascular cell basal medium were purchased from ATCC (Manassas, VA). Fetal bovine serum (FBS) was purchased from Atlanta Biologicals (Lawrenceville, GA). Penicillin and streptomycin for cell culture were purchased from Invitrogen (Grand Island, NY). HisTrap HP His tag protein purification columns were purchased from GE Healthcare Chicago, IL). Ethanol HPLC grade was purchased from Acros Organics (Waltham, MA). Yeast extract, tryptone, and kanamycin for bacterial culture were purchased from Alfa Aesar (Haverville, MA). DSPE-PEG-Maleimide linker (PG2-DSML-2k) was purchased from Nanocs (New York, NY).

Bradford reagent was purachased from BioRad (Hercules, CA). Anti-CTLA-4 mouse monoclonal antibody (clone: 9H10) and mouse IL-6, IL-12, TNFα, IFNγ ELISA kits were purchased from Biolegend (San Diego, CA). SWCNTs were obtained from CHASM (Boston, MA). Female 6 weeks old BALB/cJ mice were from Jackson Laboratory (Bar Harbor, ME). Diodevet-50 NIR laser was from B&W Tek Inc.(Newark, DE).

2.2. Methods

2.2.1. Annexin V production

E. coli BL21(DE3) was previously transformed with a plasmid ANXA5, pET-30 Ek/LIC/ANX encoding annexin V marked with a polyhistidine-tag (His-tag) and containing a kanamycin resistance gene. The gene coding for the His-tag-marked annexin V is also regulated by a Lac regulatory construct. In the presence of IPTG, this gene is activated, and recombinant annexin V is produced. First, transformed E. coli BL21(DE3) are cultivated in 10 mL of LB media containing 35 µg/mL of kanamycin at 37°C, 200 rpm shaking and for 12 hours for initial culture. The 10 mL of initial culture are then transferred in 1 L of LB media containing 35 µg/mL of kanamycin. The 1 L culture is spread into four Erlenmeyer flasks containing 250 mL of seeded medium each, and incubated for bacterial growth at 37°C, 200 rpm shaking. Each hour, the optical density of the media is measured at 600 nm using a spectrophotometer. Once the optical density at 600 nm reached 0.5, 0.4 mM of IPTG is added to each 250 mL Erlenmeyer flask of culture for the induction. Induction is performed at 30°C, 180 rpm shaking for 5 hours. The recombinant annexin V is produced intracellularly and needs to be extracted and purified from the other proteins and contaminants. Bacteria are harvested by

centrifugation at 1000g, 4°C, for 10 minutes. Supernatant is discarded, and the pellet is resuspended in a sonication buffer containing 1% ethanol, 0.05 mM of TPCK, 1 mM of PMSF and 0.02 M of sodium phosphate dibasic. The 4°C temperature, and the TPCK and PMSF (both proteases inhibitors) ensure the stability and the protection of the recombinant annexin V. β-mercaptoethanol (0.01%) is also added to the sonication buffer to prevent protein oxidation. Once fully resuspended in the sonication buffer, the cells are sonicated at 4°C for 30 seconds and 4.5 watts, then 30 seconds of pause, to break the cells membranes and release the intracellular proteins. This cycle was repeated four times. Soluble and non-soluble proteins and cell wastes are then separated by centrifugation during 30 minutes, at 12,000g and 4°C. The pellet is discarded and 40 mM of imidazole and 500 mM of NaCl is added to the supernatant. The annexin V is then purified via a nickel chromatography column. The polyhistidine-tag attached to the recombinant annexin V is trapped within the column by interacting with the Ni-NTA resin. Imidazole and NaCl are added to the supernatant to reduce unspecific binding. Annexin V is then eluted by feeding a buffer containing high concentration of imidazole (500 mM) through the column. The flowthrough is collected, and the polyhstidine-tag is then cleaved by a HRV3C protease (10U/mg of protein). A complete protocol is available in Appendix A. The amount of protein produced is then determined with a Bradford Assay. In the presence of protein, the Bradford assay reagent forms a complex with a high 595 nm absorbance. This absorbance is measured by a spectrophotometer and is proportional to the amount of protein in the sample. For each samples of annexin V produced, 5 µL were added to 96 wells containing 250 µL of Bradford reagent. The absorbance is then read within 15 minutes at 595 nm with a spectrophotometer

2.2.2. SWCNT-annexin V conjugation

SWCNTs (6 mg) were solubilized in 5 mL of 1% SDS. The solubilized SWCNTs were sonicated for 30 minutes at 6.5 watts and then centrifugated at 14,000g for 30 minutes. This cycle was repeated four times. DSPE-PEG-MAL linker (1.5 mg) solubilized in 1 mL of 1% SDS was then added, and the suspension was slowly stirred for 30 minutes at room temperature. During this step, hydrophobic interactions occurs between the SWCNTs and the DSPE functional groups of the linker. The SWCNT-linker suspension was then dialyzed for 8 hours against 2 L of DI water using a 2kDa dialysis membrane to remove unconjugated linkers and excess SDS. Annexin V (1 mL at 5mg/mL) was added to 2 mL of the SWCNT-linker suspension and slowly agitated for 2 hours at room temperature. Annexin V has one cysteine in its amino acid sequence. During this step, the sulfhydryl group of the cysteine reacts with the maleimide of the linker to form a thioether bond. This reaction is shown in **Figure 5**:

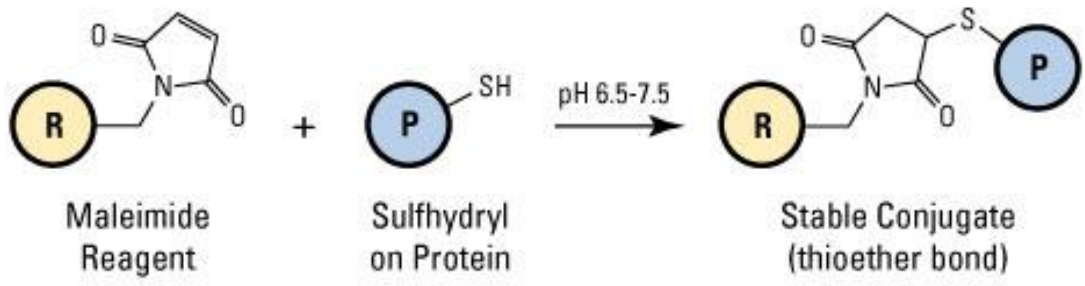

Figure 5: Maleimide conjugation reaction to a sulfhydryl group [52]. The maleimide of the DSPE-PEG-MAL linker reacts with the sulfhydryl group of the cysteine of the annexin V to form an irreversible thioether bond at a pH of 6.5 to 7.5.

The unreacted sites on the linkers were blocked by adding 0.166 mg of L-cysteine and slowly shaking for 1 hour at room temperature. The SWNCT-anx V suspension was dialyzed against 2 L of 20 mM sodium phosphate buffer at pH 7.4 during 8 hours at 4°C

using a 100 kDa dialysis membrane to remove unconjugated annexin V and excess L-cysteine. As a last step, the SWNCT-anx V suspension was centrifuged at 14,000g for 1 hour to remove the aggregates.

2.2.3. Cell culture

EMT6 cells were grown in Waymouth's MB 752/1 medium with 2 mM L-glutamine complemented with 15% FBS, penicillin (100 U/mL) and streptomycin 100 µg/mL. Cell growth was performed inside of an incubator at 37°C, 5% CO_2. EMT6 cells are highly invasive mice triple negative breast cancer cells frequently used for *in vivo* studies in mice. Their ability to metastasize quickly makes these cells a relevant model for our study. In addition, as our conjugate will be injected intravenously, human umbilical vein endothelial cells (HUVEC) was used as a control to assess the effect of the treatment on healthy cells.

2.2.4. In vitro SWCNT-annexin V based photothermal therapy

EMT6 cells were seeded in 24 well plates at a density of 20,000 cells per well. One well out of two was left empty to limit heat transfer between wells and to make sure the temperature measurements of a well will be independent from the measurement of the next one. After 48 hours, the media in each well was replaced with fresh media containing 2 mM of $CaCl_2$ and UV-sterilized SWNT-anx V conjugate and incubated at 37°C, 5% CO_2 for 2 hours. During this incubation period, the conjugate binds to phosphatidylserine exposed on the surface of the cancer cells. After the incubation period, the media is removed, and each well is washed with 300 µL of PBS. This washing step is repeated four times to remove the excess SWNT-anx V not bound to the cells. Cells were then irradiated with a Diodevet-50 NIR laser at 980 nm. The power density used was 1 W/cm². Depending on the experiment, the irradiation was performed at room temperature, or

inside of an incubator at 37°C to mimic physiological temperatures. Right after the experiment, the media is removed under a biosafety hood in sterile conditions and replaced with 250 µL of fresh media containing 10% AlamarBlue. The AlamarBlue reagent is a non-toxic dye also called resazurin. Resazurin is irreversibly reduced to a pink, fluorecent compound in proportion to aeorbic respiration. The cells are incubated for 1 to 4 hours at 37°C, 5% CO_2 until the color of the media of the control wells turned pink. The media in each wells was transferred to an opaque, black, 96 well plate and the fluorescence of each wells was measured (excitation at 530 nm and emission at 590 nm). The fluorescence of the control is used to normalize the results (average absorbance of the controls wells is set at 100% viability) and the relative viability in each well is calculated. The viability assay is performed in sterile conditions, which does not allow a thermocouple to be present in the well. For this reason, in a separate experiment, at the end of the irradiation of each wells, the cap of the plate is removed and the temperature at the bottom of the well is measured using a type j surface thermocouple.

2.2.5. In vivo SWCNT-annexin V based photothermal therapy

All the *in vivo* experiments described in this section were approved by the by Institutional Animal Care and Use Committee (IACUC) of the University of Oklahoma, and were performed by a staff with proper veterinarian training. Female 6 weeks old BALB/cJ mice were used as a model. Tumor induction was performed by orthotopic injection of 10^6 EMT6 cells in 100 µl of PBS in the fourth mammary fat pat. After 12 days post tumor induction, mice received intravenous injections of SWCNT-annexin V (1.2 mg of conjugate per kg of body mass) in the lateral tail vein. In a separate experiment, mice were also injected intratumorally to compare the effects of intratumoral and intravenous

injections. Mice were then treated with an NIR laser 3 hours after the SWCNT-anx V conjugate injection. A region with a diameter corresponding to the diameter of the tumor + 5 mm was treated. The laser wavelength was 980 nm, the power level was 1 W/cm² and the irradiation time was 175 seconds. Tumor temperature was monitored during the irradiation using a FLIR I7 thermal camera. During the irradiation, mice were anesthetized with 98% oxygen / 2% isoflurane via a nose cone. Seven days post photothermal therapy, the mice were euthanized via CO_2 with a nose cone followed by a bilateral thoracotomy. Following bilateral thoracotomy, blood was collected via intra-cardiac puncture using a 3 mL syringe. Thirty minutes post blood collection, the blood was centrifugated for 15 minutes at 14,000g, the serum was then collected and stored at 4°C.

2.2.5. In vivo SWCNT-annexin V based photothermal therapy

Statistically significance differences of cell viability and cytokine concentration were assessed using a one-way ANOVA and Tukey-Kramer multiple comparisons test with RStudio software or GraphPad Prism software version 9.0.

Chapter 3: Results

3.1. SWCNT-annexin V conjugate and properties:

Recombinant annexin V with a molecular weight of 36.5 KDa was produced in *E. coli* and purified with nickel chromatography columns. The annexin V / SWCNT ratio of the conjugate was determined by spectrophotometry. The concentration of annexin V was determined by measuring the absorbance of the conjugate after a Bradford assay at 595 nm, and the concentration of SWCNT was determined by measuring the absorbance of

the conjugate at 800 nm. As a control, absorbance at 595 nm of a DSPE-PEG-MAL linker-SWCNT conjugate (without annexin V) was measured and shown that the conjugate does not absorb at 595 nm in absence of annexin V. Absorbance at 800 nm of unconjugated annexin V was also measured to show that annexin V does not absorb at 800 nm. The average annexin V / SWCNT ratio of the different batches of conjugates used for the *in vitro* experiments presented in this thesis was 28.7 (with a minimum ratio of 22.1 and a maximum ratio of 35.4).

The photothermal effect of the SWCNT-anx V conjugate was assessed by NIR laser irradiation at 980 nm and 1 W/cm² during different times. As a control, PBS and Waymouth media were also irradiated with the laser during the same durations. The final temperature of the tested suspensions and solutions were measured at the end of the NIR irradiation and are shown in **Figure 6**:

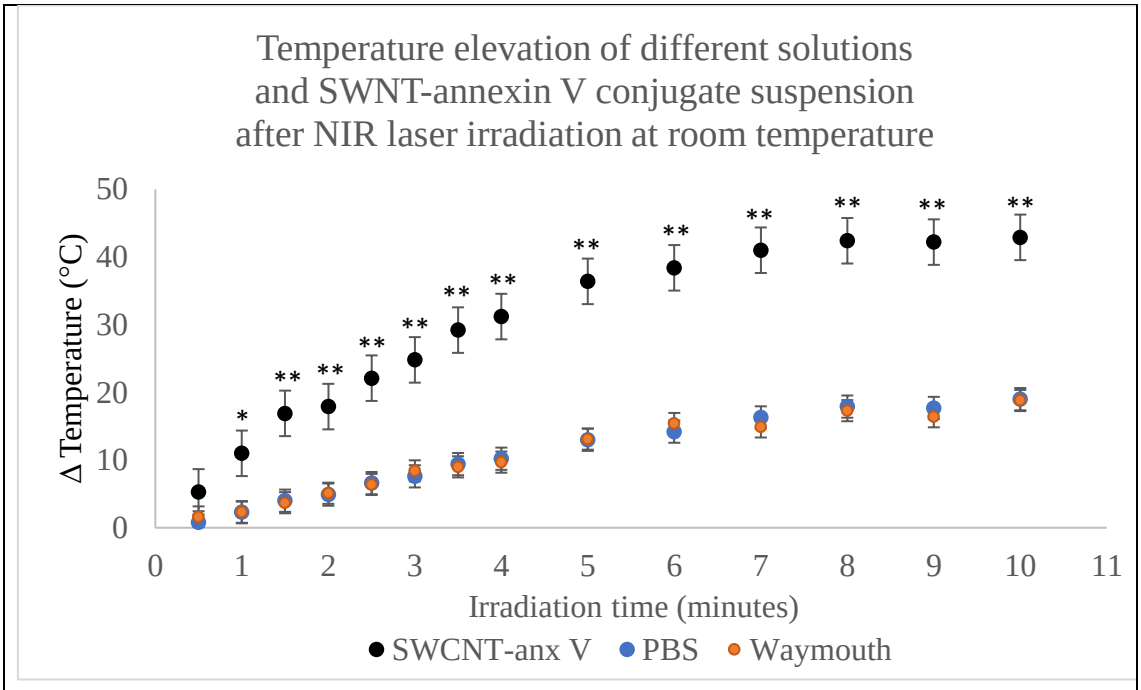

Figure 6: Temperature elevation of different solutions and SWCNT-annexin V conjugate suspension after NIR laser irradiation at room temperature.

The graph shows the increase in temperature (°C) of 1 mL of conjugate (100 mg/L), PBS or Waymouth medium as a function of irradiation time (min). Laser wavelength was 908 nm and power density 1.5 W/cm². One-way ANOVA was carried out on the R Studio software. (n = 2, *p<0.05 and **p<0.01).

The SWCNT-anx V suspension showed a significantly higher temperature elevation at room temperature compared to PBS and Waymouth media. After 8 minutes of irradiation, temperature elevation reached a plateau at $\Delta T = 42.5°C$ on average while PBS and Waymouth media reached a plateau at $\Delta T = 17.8°C$. These data suggest that the laser by itself induces a temperature elevation, but that the temperature elevation is significantly higher when the laser irradiation is combined with SWCNT-anx V conjugate. For example, after 1.5 minutes of treatment, the average temperature elevation of the wells filled with SWCNT was 16.9°C. For the same laser irradiation, the wells filled with PBS and Waymouth media presented a temperature elevation of 3.8°C. These results suggest that the conjugate generates a significant temperature elevation that can be used for our future experiments.

3.2. *In vitro* PTT results of the SWCNT-annexin V conjugate

As a scoping experiment, EMT6 cells were grown in 24 well plates and irradiated at 980 nm, 1 W/cm² during different times at room temperature. The cells were incubated with the SWCNT-anx V conjugate prior to the NIR laser irradiation at room temperature to allow the conjugate to bind to the cells, and washed 4 times with PBS to remove excess conjugate. As a control, EMT6 cells incubated without conjugate were also irradiated. At the end of the NIR irradiation, an Alamar Blue Assay was performed to determine the viability of the EMT6 cells, and the results are shown in **Figure 7**:

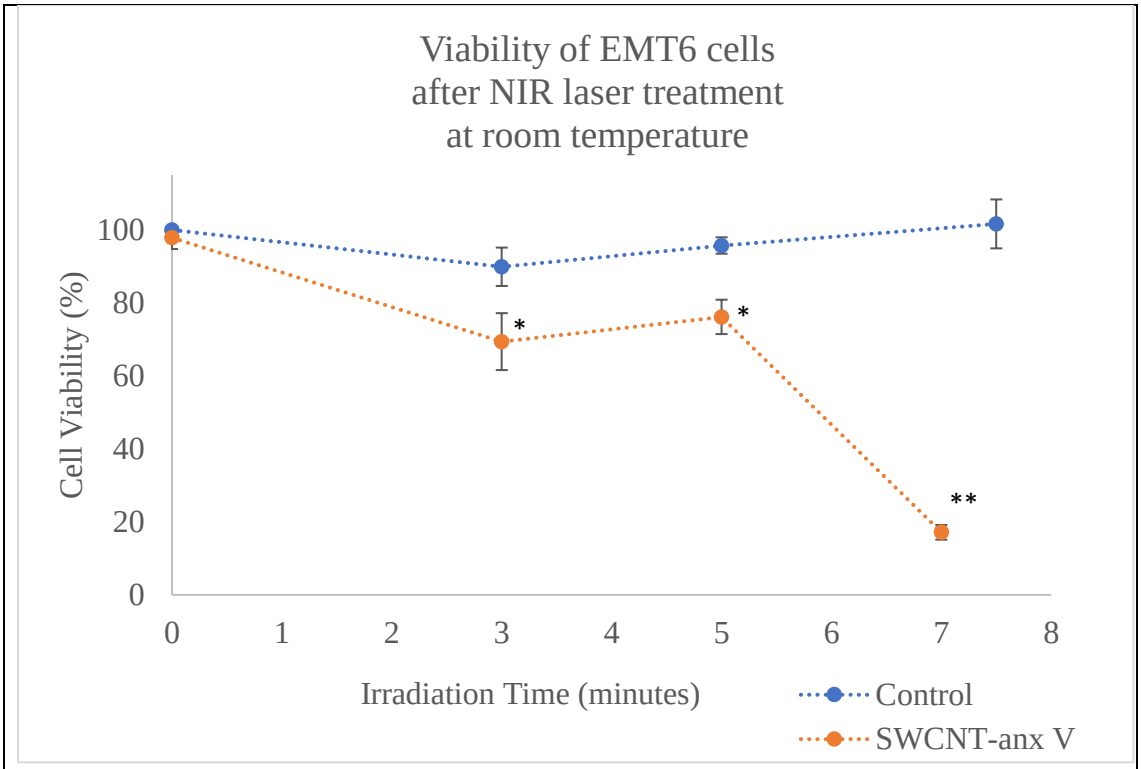

Figure 7: Viability of EMT6 cells after NIR laser treatment at room temperature. The graph shows the relative cell viability of EMT6 cells incubated for 2 hours with the conjugate (in orange) or incubated with Waymouth medium as a control (in blue), prior to laser irradiation. After incubation with the conjugate, the cells were washed four times with PBS. Laser wavelength was 908 nm and power density 1.0 W/cm². One-way ANOVA was carried out on the R Studio software. (n = 2-3, *$p<0.05$ and **$p<0.01$).

At room temperature, the treatment showed a significant drop in cell viability after 3 minutes of irradiation. The control consisted of EMT6 cells irradiated with the laser in absence of SWCNT-anx V conjugate and did not present a trend of viability drop between 1 to 7 minutes of laser irradiation. After 7 minutes of irradiation, the EMT6 cells incubated with the conjugate presented a viability of 17% on average. In this experiment, the treatment at room temperature seemed to show a tendency to decrease the cell viability

of the cancer cells exposed to the conjugate while the laser alone had no effect on the cell viability.

In a separate experiment, instead of measuring the cell viability at the end of the NIR irradiation at room temperature, the final temperature at the bottom of the well plate was measured using a type j thermocouple. This experiment makes it possible to determine the temperature rise induced by the PTT. The temperature rises resulting from the PTT are shown in **Figure 8**:

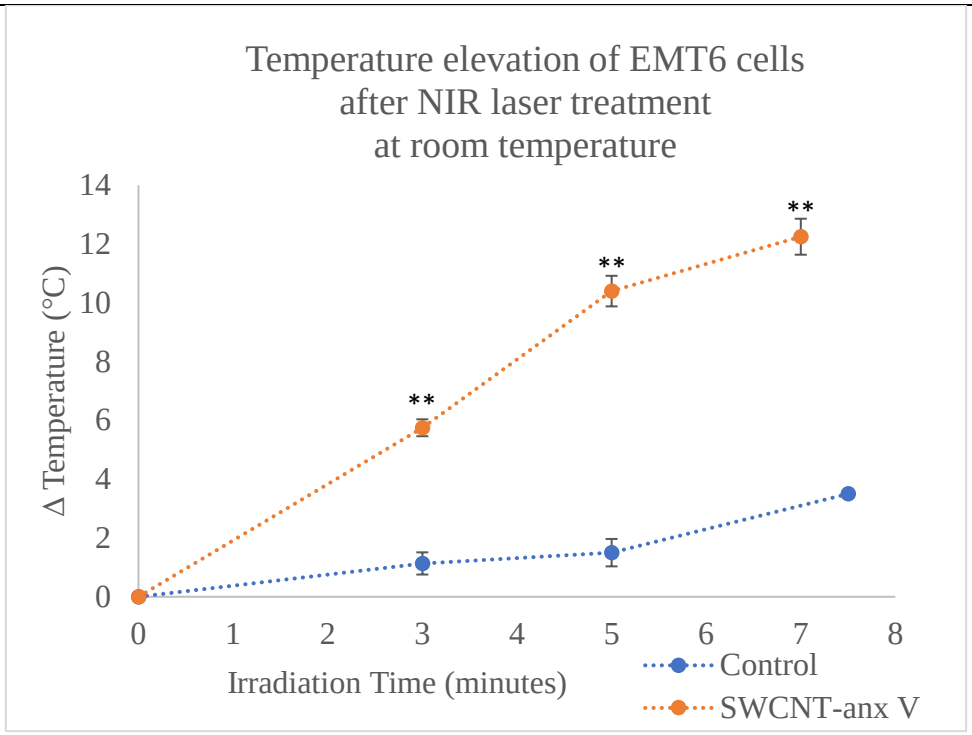

Figure 8: Temperature elevation of EMT6 cells after NIR laser treatment at room temperature. The graph shows the temperature elevation (°C) of EMT6 cells incubated for 2 hours with the conjugate (in orange) or incubated with Waymouth medium as a control (in blue), prior to laser irradiation. After incubation with the conjugate, the cells were washed four times with PBS. Laser wavelength was 908 nm and power density 1.0 W/cm². One-way ANOVA was carried out on the R Studio software. (n = 2-3, *$p<0.05$ and **$p<0.01$).

EMT6 cells treated with SWCNT-anx V conjugate and PTT showed an increased temperature elevation compared to the control treated with laser irradiation alone. These results suggest that the laser alone does not induce a strong rise in temperature, and that the combination of laser and conjugate is necessary to induce significant heat.

The previous *in vitro* experiments were performed at room temperature and gave preliminary results on the effect of a PTT using the SWCNT-anx V conjugate on a TNBC model. However, one could argue that EMT6 cells may not react the same at room temperature as they do at a physiological temperature of 37 ° C. In order to determine if it is the case, a separate experiment was carried out at 37 ° C in an incubator. At the end of the NIR irradiation inside of the incubator, an Alamar Blue Assay was performed to determine the viability of the EMT6 cells, and the results are shown in **Figure 9**:

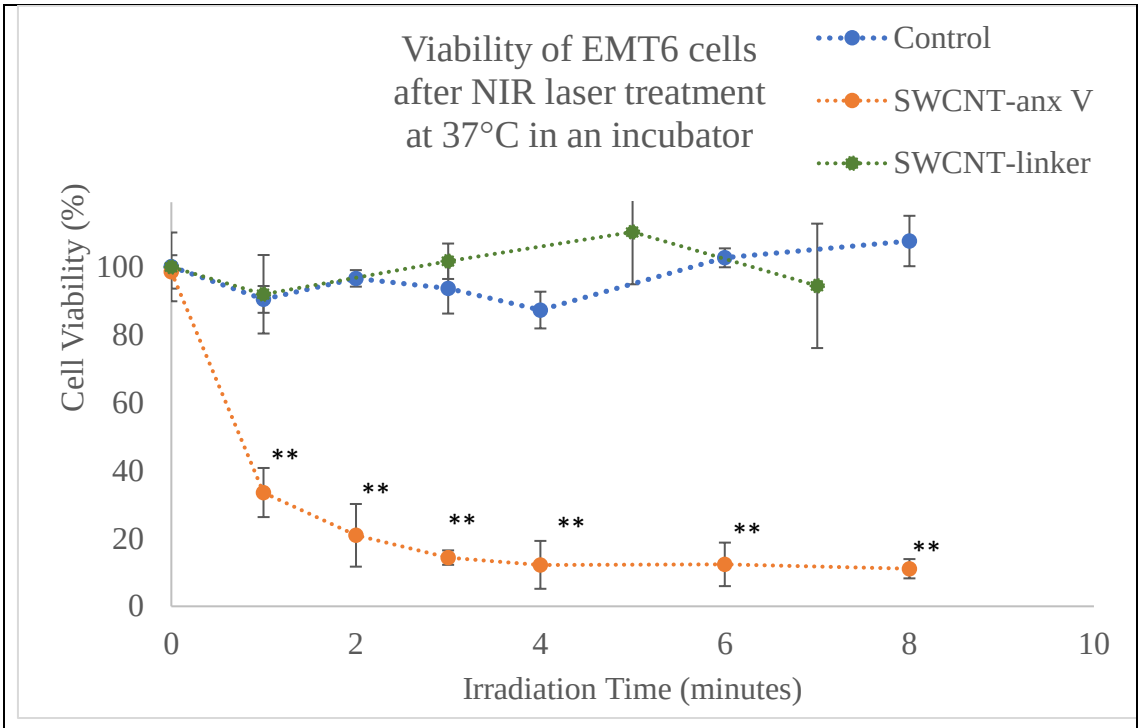

Figure 9: Viability of EMT6 cells after NIR laser treatment at 37°C in an incubator. The graph shows the relative cell viability of EMT6 cells incubated for 2 hours with the conjugate (in orange), or incubated with Waymouth medium as a control

(in blue), or incubated with nanotubes conjugated to the linker only (in green), prior to laser irradiation. After incubation with the conjugate, the cells were washed four times with PBS. Laser wavelength was 908 nm and power density 1.0 W/cm². One-way ANOVA was carried out on the R Studio software. (n = 3, *p<0.05 and **p<0.01).

EMT6 cells treated with both SWCNT-anx V conjugate and laser irradiation showed a significant cell viability drop after 1 minute of irradiation. The cell viability drop reached a relative plateau after 3 minutes of laser irradiation at 14% cell viability on average. This result suggests that the optimal time of irradiation to treat EMT6 cells at 37°C is located between 2 and 3 minutes of laser irradiation.

Comparatively, cells treated with laser alone, or SWNCT-linker (without Anx V) conjugate and laser did not result in a significant cell viability drop even after 7 minutes of laser irradiation. These results strongly suggest that Anx V is necessary for the conjugate to bind to the cells. After four washing steps, untargeted conjugate is washed away from the wells, and only the targeted conjugate induces a photothermal effect after laser irradiation *in vitro* at 37°C.

In order to verify that the conjugate does not affect healthy cells, a separate experiment was performed using HUVEC cells as a model. HUVEC cells were grown in 24 wells plates until reaching confluency, and were then treated with laser irradiation alone at 37°C, or laser irradiation at 37°C combined with SWCNT-anx V treatment. The results are shown in **Figure 10**:

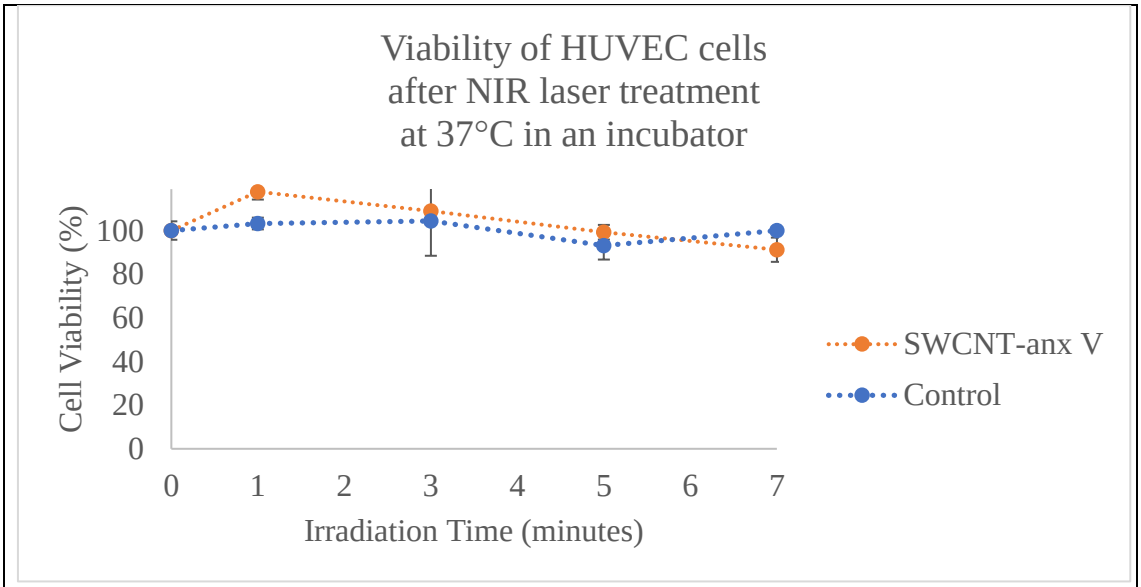

Figure 10: Viability of HUVEC cells after NIR laser treatment at 37°C in an incubator. The graph shows the temperature elevation (°C) of HUVEC cells incubated for two hours with the conjugate (in orange) or incubated with VCBM medium as a control (in blue), prior to laser irradiation. After incubation with the conjugate, the cells were washed four times with PBS. Laser wavelength was 908 nm and power density 1.0 W/cm². One-way ANOVA was carried out on the R Studio software. (n = 3, *p<0.05 and **p<0.01).

After 7 minutes of treatment, neither the group treated with SWCNT-anx V nor the group treated with laser irradiation alone showed a significant cell viability drop. In physiological conditions, healthy confluent endothelial cells do not express phosphatidylserine externally [53]. These results suggest that the SWCNT-anx V conjugate is not able to bind confluent healthy endothelial cells, and therefore, is not able to induce a photothermal effect to these cells after laser irradiation.

3.3. *In vivo* PTT results of the SWCNT-annexin V conjugate in mice model

Female BALB/cJ mice bearing EMT6 tumors were treated with intravenous injection of SWCNT-anx V in the lateral tail vein or intratumoral injections of the conjugate. The tumor was then treated by photothermal therapy. The temperature of the tumor was monitored during the laser irradiation using an IR camera. Seven days post photothermal therapy, the mice were euthanized, blood samples were gathered and centrifuged to collect the serum, and enzyme-linked immunosorbent assays were performed to quantify levels of TNFα in the serum. Mice treated with intravenous injections of SWCNT-anx V and photothermal therapy for 175 seconds presented significantly increased serum levels of TNFα ($p<0.05$). Mice treated with intratumoral injections of SWCNT-anx V combined with PTT for 175 seconds showed even more significant increased levels of TNFα in the serum compared to the control ($p< 0.0001$). Results are shown in **Figure 11**.

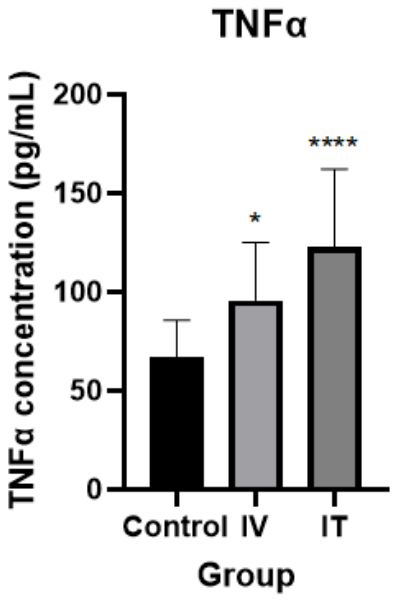

Figure 11: TNFα concentrations in serum 24 hours after PTT in mice treated with IV injection or IT injection of the conjugate. The diagram shows the level of TNFα in the serum of mice treated with intravenous (IV) or intratumoral (IT) injections of

conjugate, or untreated mice as a control. Laser wavelength was 908 nm and power density 1.0 W/cm². Blood samples were collected 24 hours after photothermal therapy. One-way ANOVA and Dunnett's multiple comparisons were carried out on the Graphpad Prism software version 9.0. (n = 4-5, *p<0.05, and ****p<0.0001)

In a separate experiment, mice were treated with intratumoral injections of the conjugate combined with photothermal therapy until a final tumor temperature of 45, 50, 55 or 60°C was reached, and the concentration of four cytokines was measured in the serum 1 and 7 days after PTT. The results are shown in **Figure 12**.

Mice with final tumor temperatures of 45, 50 or 60°C showed significantly increased levels of TNFα in the serum 1 day after PTT compared to the control and increased levels of TNFα in the serum 7 days after PTT for tumor final temperatures of 45°C and 55°C. The treatment reaching a final temperature of 60°C also induced a significant release of IL-6 in the serum of the mice 1 day after PTT. The treatment did not induce increased levels of Il-12(p70) and IFNγ in the serum 1 day and 7 days after PTT, and the treatment did not induce increased levels of IL-6 in the serum 7 days after PTT.

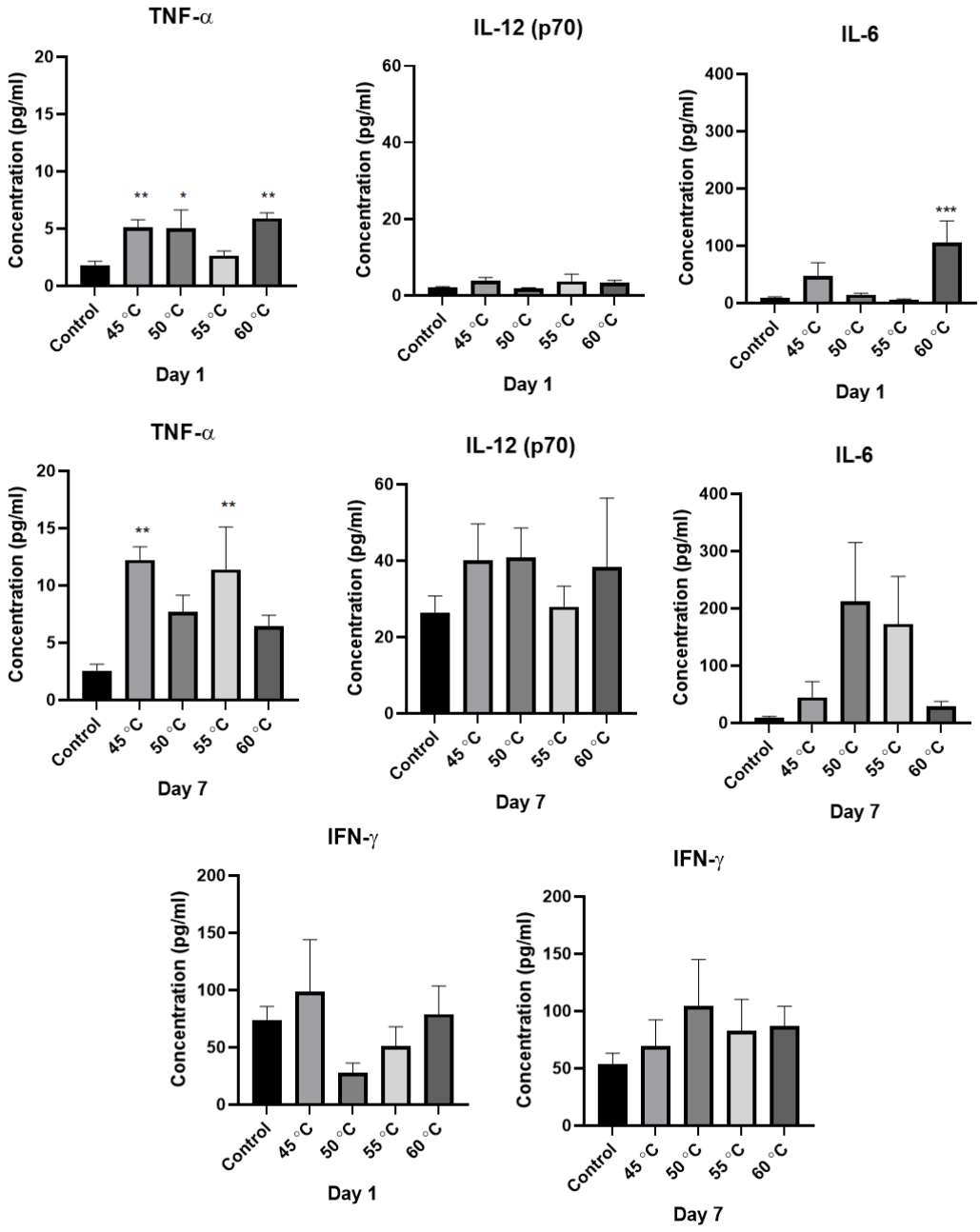

Figure 12: Cytokine concentrations in serum 1 day and 7 days after PTT with different final temperatures. The diagram shows the level of TNFα, IL-6, IL-12(p70) and IFNγ in the serum of mice treated with IT injections of conjugate, or untreated mice as a control. Photothermal therapy was performed until reaching a final temperature of 45, 50, 55, or 60°C. Laser wavelength was 908 nm and power density 1.0 W/cm². Blood samples were collected 1 day or 7 days after photothermal therapy.

For each treatment compared to the control, one-way ANOVA and Dunnett's multiple comparisons were carried out on the Graphpad Prism software version 9.0.
(n = 4-5, *p<0.05, **p<0.01 and ***p<0.001)

In recent work in our laboratory and following the same procedures, Patrick McKernan and Needa Virani treated BALB/cJ mice bearing EMT6 tumors with SWCNT-anx V and photothermal therapy [54]. This treatment was combined with administration of a checkpoint inhibitor; anti-CTLA-4, to the mice 8, 11, and 16 days post tumor inoculation. McKernan and Virani notably showed an increased survival of 55% in the group treated with both SWCNT-anx V photothermal therapy and anti-CTLA-4 at 100 days post tumor inoculation [53].

Comparatively, no survival at 100 days was observed in the group treated with SWCNT-anx V photothermal therapy alone, as well as in the group treated with anti-CTLA-4 alone [54]. In order to strengthen this pre-existing work and to highlight the abscopal effect induced by the treatment, we performed a quantification of proinflammatory cytokines present in the serum. BALB/cJ mice were treated following the same procedure, and separated in five groups (n = 5 in each group):

1) Untreated control group (control).

2) Mice treated with SWNT-Anx V injections, but not treated with photothermal therapy (SWNT).

3) Mice treated with both SWNT-Anx V injections and photothermal therapy (SWNT+PTT).

4) Mice treated with anti-CTLA-4 treatment alone (anti-CTLA-4).

5) Mice treated with SWNT-Anx V injections, photothermal therapy, and anti-CTLA-4 (SWNT+PTT+anti-CTLA-4).

Seven days post photothermal therapy, mice were euthanized, blood samples were taken and centrifugated to collect the serum, and enzyme-linked immunosorbent assays were performed to quantify serum levels of IFNγ, TNFα and IL6. A standard curve was performed for each cytokine to determine the concentration of IFNγ, TNFα and IL6 in the serum samples. These standard curves are available in Appendix C. Serum levels of IFNγ, TNFα and IL6 are shown in **Figure 13**:

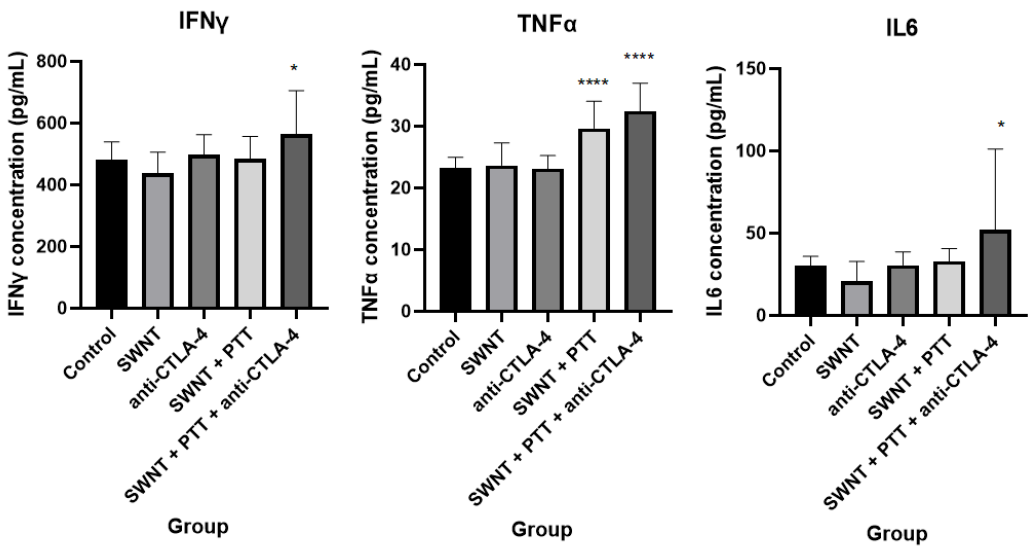

Figure 13: Cytokine concentrations in serum 7 days after PTT in mice treated with anti-CTLA4. The diagram shows the level of IFNγ, TNFα and IL-6 in the serum of mice treated with IT injections of conjugate, anti-CTLA-4 injection alone, IT injections of conjugate combined with PTT, IT injections of conjugate combined with PTT and anti-CTLA4 injection, or untreated mice as a control. Laser wavelength was 908 nm and power density 1.0 W/cm² for 175 seconds. Blood samples were collected 7 days after photothermal therapy. For each treatment compared to the control, one-way ANOVA and Dunnett's multiple comparisons were carried out on the Graphpad

Prism software version 9.0. (n = 4-5, *p<0.05, and ****p<0.0001)

Mice treated with anti-CTLA-4 alone or SWCNT-anx V injections alone did not give any significant increase of proinflammatory cytokines in the serum compared to the untreated control. Mice treated with the combination of SWCNT-anx V injections, photothermal therapy and anti-CTLA-4 injections gave significantly increased serum levels of IFNγ, TNFα and IL6 compared to the control, while mice treated with the combination of SWCNT-anx V injections and photothermal therapy gave significantly increased serum levels of TNFα compared to the control.

An improvement in the overall health status of mice treated with targeted photothermal therapy coupled with injections of anti-CTLA-4 was observed within 7 days following photothermal therapy. During this post-treatment period, the mice treated with targeted photothermal therapy coupled with injections of anti-CTLA-4 moved around the entire cage, playing with the wooden cubes placed at their disposal. In comparison, mice in the control group remained immobile in a corner of the cage.

Chapter 4: Discussion

Triple negative breast cancer represents a strong clinical challenge due to the lack of targeted therapies [13-15]. An improved overall survival has been demonstrated in patients treated with radiation therapy in addition to chemotherapy and surgery [23-25], highlighting the importance of radiation therapy in the treatment of triple negative breast cancer.

Our work proposes the use of annexin V conjugated to carbon nanotubes in a new approach of targeted photothermal therapy to answer this unmet clinical need. This new treatment has demonstrated *in vitro* efficacy on EMT6 cells, a very aggressive and highly metastatic model of triple negative breast cancer.

Furthermore, it has been observed that annexin V is necessary for the effectiveness of the treatment. Indeed, the use of the conjugate without annexin V did not show any efficacy in vitro on an EMT6 model, suggesting that the treatment is specific and requires annexin V to bind to phosphatidylserine externalized by cancer cells. The treatment has also been shown to not induce cytotoxicity in a model of healthy endothelial cells. This information is crucial, because in the context of an intravenous injection of the conjugate, it is necessary that the treatment does not damage the endothelial cells of the vasculature. The experiments revealed that the conjugates do not appear to bind to endothelial cells, making the treatment specific to cancer cells externalizing phosphatidylserine.

The increased levels of the four serum cytokines studied suggest that the treatment induces an antitumoral immune response. IFNγ is known for playing a key role in tumor surveillance, TNFα is a tumor associated macrophages activator, and IL-6 enhances lymphocyte and macrophage proliferation. The lowest temperature studied, 45°C, gave a

significantly higher level of TNFα at both 1 and 7 days after PTT compared to the untreated control (**Figure 12**).

In recent works, Wang et al. were able to ablate a tumor reaching a final tumor temperature of 53°C using SWCNTs-based photothermal therapy [51]. Their experiments showed significantly increased levels of TNFα in serum 7 days after the treatment, similar to the results observed in our experiment. Using indocyanine green-based photothermal therapy, Chen et al. performed tumor ablation in mice and reached a final tumor temperature of 60°C [55]. Their experiments showed no significantly increased levels of IL-12 and IL-6 in serum 1 and 7 days after the treatment, which was similar to the results observed in our experiment. However, Chen et al. also measured the levels of IL-6 and IL-12 in serum 3 days after the treatment [56]. Significant increased levels of IL-12 and IL-6 in serum were measured, suggesting that the peak release of IL-12 and IL-6 is around 3 days after the treatment. Although our experiments showed a significantly increased level of IL-6 in serum 1 day after the treatment when reaching a tumor final temperature of 60°C, 3 days may be a more suitable time to quantify Il-6 and IL-12 release after photothermal therapy.

The data on the effect of adding anti-CTLA-4 to PTT show that this resulted in significantly increased levels of cytokines IFNγ, TNFα and IL-6 compared to treatment with SWCNTs, anti-CTLA-4, or PTT alone (**Figure 13**). For these experiments, PTT was performed for 175 seconds, which we previously found to give a final tumor temperature of 54°C for EMT6 tumors in mice [54]. These data on cytokine release support the abscopal effect that we previously found, where a significant survival was obtained, as well as a significant increase in the relative numbers of cytotoxic and helper T cells, for the

combination of PTT and anti-CTLA-4 administration but no survival with anti-CTLA-4 alone [54].

Chapter 5: Conclusions

Annexin V was successfully conjugated to SWCNTs using a DSPE-PEG-MAL linker. The conjugate showed a photothermal effect, and the increase in temperature following photothermal therapy significantly reduced the cellular viability of EMT6 cells at room temperature as well as at 37 ° C. In the absence of annexin V, the conjugate was unable to induce significant cell death. This result suggests that the annexin V is indeed necessary for the use an SWNCTs conjugate for targeted photothermal therapy.

The conjugate also demonstrated that it does not induce significant cell death after photothermal therapy on healthy endothelial HUVEC cells, suggesting that the conjugate is only able to bind to the cells externalizing the phosphatidylserine. *In vivo* experiments have demonstrated the ability of treatment to induce an increase in the level of proinflammatory cytokines in the mice bloodstream. These results support the hypothesis previously put forward that the treatment induces an abscopal effect, and that the treatment could be used in the treatment of triple negative breast cancer metastases.

Future directions:

For the study of the effect of tumor temperature on the release of cytokines, there was considerable variability in the data (Figure 12). Cytokine research did not always increase as temperature increased. Therefore, to reduce this variability, the number of animals per group should be increased, possibly doubling from n = 4-5 per group to n = 8-10 per group.

In addition, it would be interesting to measure the release of IL-6 and IL-12 in the serum 3 days after the photothermal therapy to be closer to the peak of release of these cytokines.

The NIR laser light used for this treatment is rapidly attenuated by biological tissues, making the treatment of deep tumors more complicated. In order to address this problem, the conjugate could be activated using a radiofrequency generator. Indeed, radiofrequency fields are commonly used in biomedical imaging for their properties to penetrate biological tissues. In previous work in this lab, the conjugate has already demonstrated absorbance in a radiofrequency field with a frequency of 13.56MHz, and future work in this area could allow the development of a noninvasive targeted photothermal therapy based on radiofrequencies and an SWCNT-anx V conjugate.

Furthermore, triple negative breast cancer was used as a model in this research, but this prototype could be also used for other types of cancer externalizing phosphatidylserine.

References

[1]: Dorn, C. R., & Priester, W. A. (1976). Epidemiologic analysis of oral and pharyngeal cancer in dogs, cats, horses, and cattle. *Journal of the American Veterinary Medical Association*, *169*(11), 1202–1206.

[2]: Hollstein, M., Sidransky, D., Vogelstein, B., & Harris, C. (1991). P53 mutations in human cancers. *Science*, *253*(5015), 49–53.

[3]: Khanna, C., Lindblad-Toh, K., Vail, D., London, C., Bergman, P., Barber, L., Breen, M., Kitchell, B., McNeil, E., Modiano, J. F., Niemi, S., Comstock, K. E., Ostrander, E., Westmoreland, S., & Withrow, S. (2006). The dog as a cancer model. *Nature Biotechnology*, *24*(9), 1065–1066.

[4]: Medhurst, S. J., Walker, K., Bowes, M., Kidd, B. L., Glatt, M., Muller, M., Hattenberger, M., Vaxelaire, J., O'Reilly, T., Wotherspoon, G., Winter, J., Green, J., & Urban, L. (2002). A rat model of bone cancer pain. *Pain*, *96*(1), 129–140.

[5]: Velcich, A. (2002). Colorectal Cancer in Mice Genetically Deficient in the Mucin Muc2. *Science*, *295*(5560), 1726–1729.

[6]: Minn, A. J., Gupta, G. P., Siegel, P. M., Bos, P. D., Shu, W., Giri, D. D., Viale, A., Olshen, A. B., Gerald, W. L., & Massagué, J. (2005). Genes that mediate breast cancer metastasis to lung. *Nature*, *436*(7050), 518–524.

[7]: Nguyen, D. X., & Massagué, J. (2007). Genetic determinants of cancer metastasis. *Nature Reviews Genetics*, *8*(5), 341–352.

[8]: Poste, G., & Fidler, I. J. (1980). The pathogenesis of cancer metastasis. *Nature*, *283*(5743), 139–146.

[9]: Detterbeck, F. C., Boffa, D. J., Kim, A. W., & Tanoue, L. T. (2017). The Eighth Edition Lung Cancer Stage Classification. *Chest*, *151*(1), 193–203.

[10]: Cleator, Susan, Wolfgang Heller, and R Charles Coombes. 2007. ‘Triple-Negative Breast Cancer: Therapeutic Options’. The Lancet Oncology 8(3): 235–44.

[11]: Dent, Rebecca et al. 2007. ‘Triple-Negative Breast Cancer: Clinical Features and Patterns of Recurrence’. Clinical Cancer Research 13(15): 4429–34.

[12]: Hudis, Clifford A., and Luca Gianni. 2011. ‘Triple-Negative Breast Cancer: An Unmet Medical Need’. The Oncologist 16(S1): 1–11.

[13]: Voduc KD, Cheang MC, Tyldesley S, Gelmon K, Nielsen TO, Kennecke H. Breast cancer subtypes and the risk of local and regional relapse. J Clin Oncol. 28(10):1684-91, 2010.Van der Zee, J. 2002. ‘Heating the Patient: A Promising Approach?’ Annals of Oncology 13(8): 1173–84.

[14]: Kohler BA, Sherman RL, Howlader N, et al. Annual report to the nation on the status of cancer, 1975- 2011, featuring incidence of breast cancer subtypes by race/ethnicity, poverty, and state. J Natl Cancer Inst. 107(6), 2015.

[15]: Anders CK, Carey LA. ER/PR negative, HER2-negaitve (triple negative) breast cancer. In: UpToDate. Hayes DF, Vora SR (eds.). Waltham, MA: UpToDate, 2019.

[16]: Freedman, Gary M., Penny R. Anderson, Tianyu Li, and Nicos Nicolaou. 2009. ‘Locoregional Recurrence of Triple-Negative Breast Cancer after Breast-Conserving Surgery and Radiation’. Cancer 115(5): 946–51.

[17]: Steward, Lauren T., Feng Gao, Marie A. Taylor, and Julie A. Margenthaler. 2014. ‘Impact of Radiation Therapy on Survival in Patients with Triple negative Breast Cancer’. Oncology Letters 7(2): 548– 52.Foulkes, William D., Ian E. Smith, and Jorge S. Reis-Filho. 2010. ‘Triple-Negative Breast Cancer’. New England Journal of Medicine 363(20): 1938–48.

[18] Wahba, Hanan Ahmed, and Hend Ahmed El-Hadaad. 2015. ‘Current Approaches in Treatment of Triple-Negative Breast Cancer’. Cancer Biology & Medicine 12(2): 106–16.

[19]: Yagata, Hiroshi, Yuka Kajiura, and Hideko Yamauchi. 2011. ‘Current Strategy for Triple-Negative Breast Cancer: Appropriate Combination of Surgery, Radiation, and Chemotherapy’. Breast Cancer 18(3): 165–73.

[20]: Keam, Bhumsuk et al. 2007. ‘Prognostic Impact of Clinicopathologic Parameters in Stage II/III Breast Cancer Treated with Neoadjuvant Docetaxel and Doxorubicin Chemotherapy: Paradoxical Features of the Triple Negative Breast Cancer’. BMC Cancer 7(1): 203.

[21]: Zeng, Qing et al. 2010. ‘Treating Triple-Negative Breast Cancer by a Combination of Rapamycin and Cyclophosphamide: An in Vivo Bioluminescence Imaging Study’. European Journal of Cancer 46(6): 1132–43.

[22]: Sikov, William M. et al. 2015. ‘Impact of the Addition of Carboplatin and/or Bevacizumab to Neoadjuvant Once-per-Week Paclitaxel Followed by Dose-Dense Doxorubicin and Cyclophosphamide on Pathologic Complete Response Rates in Stage II to III Triple-Negative Breast Cancer: CALGB 40603 (Alliance)’. Journal of Clinical Oncology 33(1): 13–21.

[23]: Abdulkarim, Bassam S. et al. 2011. ‘Increased Risk of Locoregional Recurrence for Women With T1- 2N0 Triple-Negative Breast Cancer Treated With Modified Radical Mastectomy Without Adjuvant Radiation Therapy Compared With Breast-Conserving Therapy’. Journal of Clinical Oncology 29(21): 2852–58.

[24]: Steward, Lauren T., Feng Gao, Marie A. Taylor, and Julie A. Margenthaler. 2014. 'Impact of Radiation Therapy on Survival in Patients with Triple-Negative Breast Cancer'. Oncology Letters 7(2): 548–52.

[25]: Wang, Jianhua et al. 2011. 'Adjuvant Chemotherapy and Radiotherapy in Triple-Negative Breast Carcinoma: A Prospective Randomized Controlled Multi-Center Trial'. Radiotherapy and Oncology 100(2): 200–204.

[26]: Shakiba, M., J. Chen, and G. Zheng. 2015. '24 - Porphyrin Nanoparticles in Photomedicine'. In Applications of Nanoscience in Photomedicine, eds. Michael R. Hamblin and Pinar Avci. Oxford: Chandos Publishing, 511–26.

[27]: Zhou, Feifan et al. 2009. 'Cancer Photothermal Therapy in the Near-Infrared Region by Using SingleWalled Carbon Nanotubes'. Journal of Biomedical Optics 14(2): 021009.

[28]: Liang, Chao et al. 2014. 'Tumor Metastasis Inhibition by Imaging-Guided Photothermal Therapy with Single-Walled Carbon Nanotubes'. Advanced Materials 26(32): 5646–52.

[29]: Huang, Xiaohua, Ivan H. El-Sayed, Wei Qian, and Mostafa A. El-Sayed. 2006. 'Cancer Cell Imaging and Photothermal Therapy in the Near-Infrared Region by Using Gold Nanorods'. Journal of the American Chemical Society 128(6): 2115–20.

[30]: Liu, Huiyu et al. 2011. 'Multifunctional Gold Nanoshells on Silica Nanorattles: A Platform for the Combination of Photothermal Therapy and Chemotherapy with Low Systemic Toxicity'. Angewandte Chemie International Edition 50(4): 891–95.

[31]: Shen, Shun et al. 2013. 'Targeting Mesoporous Silica-Encapsulated Gold Nanorods for ChemoPhotothermal Therapy with near-Infrared Radiation'. Biomaterials 34(12): 3150–58.

[32]: Ji, Xiaojun et al. 2007. ‘Bifunctional Gold Nanoshells with a Superparamagnetic Iron Oxide−Silica Core Suitable for Both MR Imaging and Photothermal Therapy’. The Journal of Physical Chemistry C 111(17): 6245–51.

[33]: Dong, X., Tang, Y., Wu, M., Vlahovic, B., & Yang, L. (2013). Dual effects of single-walled carbon nanotubes coupled with near-infrared radiation on Bacillus anthracis spores: Inactivates spores and stimulates the germination of surviving spores. Journal of Biological Engineering, 7(1), 19.

[34]: Wust, P et al. 2002. ‘Hyperthermia in Combined Treatment of Cancer’. The Lancet Oncology 3(8): 487–97.

[35]: Gordon, R. T, J. R Hines, and D Gordon. 1979. ‘Intracellular Hyperthermia a Biophysical Approach to Cancer Treatment via Intracellular Temperature and Biophysical Alterations’. Medical Hypotheses 5(1): 83–102.

[36]: C. Brace, Thermal Tumor Ablation in Clinical Use, IEEE pulse, 2 (2011) 28- 38.

[37]: H.O.W. Tseng, S.-E. Lin, Y.-L. Chang, M.-H. Chen, S.-H. Hung, Determining the critical effective temperature and heat dispersal pattern in monopolar radiofrequency ablation using temperature-time integration, Experimental and Therapeutic Medicine, 11 (2016) 763-768.

[38]: McKernan, Patrick. 2018. ‘Therapeutic Applications of Bioconjugates in Human Disease’.

[39]: Ribeiro, B., Botelho, E., Costa, M., & Bandeira, C. (2017). Carbon nanotube buckypaper reinforced polymer composites: A review. *Polímeros*, *27*.

[40]: N.W.S. Kam, M. O'Connell, J.A. Wisdom, H. Dai, Carbon nanotubes as multifunctional biological transporters and near-infrared agents for selective cancer cell

destruction, Proceedings of the National Academy of Sciences of the United States of America, 102 (2005) 11600-11605.

[41]: Y. Xiao, X. Gao, O. Taratula, S. Treado, A. Urbas, R.D. Holbrook, R.E. Cavicchi, C.T. Avedisian, S. Mitra, R. Savla, P.D. Wagner, S. Srivastava, H. He, Anti-HER2 IgY antibody-functionalized single-walled carbon nanotubes for detection and selective destruction of breast cancer cells, BMC Cancer, 9 (2009) 351-351.

[42]: X. Liu, H. Tao, K. Yang, S. Zhang, S.T. Lee, Z. Liu, Optimization of surface chemistry on single-walled carbon nanotubes for in vivo photothermal ablation of tumors, Biomaterials, 32 (2011) 144-151.

[43]: N.A. Virani, P. McKernan, R.G. Harrison, Photothermal therapy using carbon nanotubes for treating cancer in: D.V. Papavassiliou, H.M. Duong, F. Gong (Eds.) Thermal Behavior and Applications of Carbon Based Nanomaterials, Elsevier, Amsterdam, 2020, pp. 325-344.

[44]: Koopman, G., Reutelingsperger, C. P., Kuijten, G. A., Keehnen, R. M., Pals, S. T., & van Oers, M. H. (1994). Annexin V for flow cytometric detection of phosphatidylserine expression on B cells undergoing apoptosis. *Blood, 84*(5), 1415–1420.

[45]: Vermes, I., Haanen, C., Steffens-Nakken, H., & Reutellingsperger, C. (1995). A novel assay for apoptosis Flow cytometric detection of phosphatidylserine expression on early apoptotic cells using fluorescein labelled Annexin V. *Journal of Immunological Methods, 184*(1), 39–

[46]: Riedl, Sabrina et al. 2011. ‘In Search of a Novel Target — Phosphatidylserine Exposed by NonApoptotic Tumor Cells and Metastases of Malignancies with Poor

Treatment Efficacy'. Biochimica et Biophysica Acta (BBA) - Biomembranes 1808(11): 2638–45.

[47]: Mariño, Guillermo, and Guido Kroemer. 2013. 'Mechanisms of Apoptotic Phosphatidylserine Exposure'. Cell Research 23(11): 1247–48.

[48]: Gray, M. J., Gong, J., Hatch, M. M. S., Nguyen, V., Hughes, C. C. W., Hutchins, J. T., & Freimark, B. D. (2016). Phosphatidylserine-targeting antibodies augment the anti-tumorigenic activity of anti-PD-1 therapy by enhancing immune activation and downregulating pro-oncogenic factors induced by T-cell checkpoint inhibition in murine triple-negative breast cancers. *Breast Cancer Research: BCR*, *18*(1), 50.

[49]: Bagarie C. P., 2018. 'Annexin a5 – Chlorambucil: a targeted therapeutic drug against leukemia and breast cancer'

[50]:.Nanocs 'DSPE PEG Maleimide, technical data sheet CAS number: 474922-22-0'

[51]: Wang, C., Xu, L., Liang, C., Xiang, J., Peng, R., & Liu, Z. (2014). Immunological Responses Triggered by Photothermal Therapy with Carbon Nanotubes in Combination with Anti-CTLA-4 Therapy to Inhibit Cancer Metastasis. *Advanced Materials*, *26*(48), 8154–8162.

[52]: Hermanson, G. T. (2013). *Bioconjugate Techniques* (Third edition). Academic Press.

[53]: Krais, J. J., Crescenzo, O. D., & Harrison, R. G. (2013). Purine Nucleoside Phosphorylase Targeted by Annexin V to Breast Cancer Vasculature for Enzyme Prodrug Therapy. PLOS ONE, 8(10), 8.

[54]: McKernan, P., Virani, N. A., Nogueira Furtado E Faria, G., Karch, C. G., Silvy R. P., Resasco, D. E., Thompson, L. F., Harrison, R. G. (accepted 2020) 'Targeted Single-

Walled Carbon Nanotubes for Photothermal Therapy Combined with Immune Checkpoint Inhibition for the Treatment of Metastatic Breast Cancer'. *Nanoscale Research Letters.*

[55]: Wang, C., Xu, L., Liang, C., Xiang, J., Peng, R., & Liu, Z. (2014). Immunological Responses Triggered by Photothermal Therapy with Carbon Nanotubes in Combination with Anti-CTLA-4 Therapy to Inhibit Cancer Metastasis. Advanced Materials, 26(48), 8154–8162.

Appendix

List of Appendix:

Appendix A: Annexin V production and purification protocol

Protocol from Charles Bagarie, source: *Bagarie C. P., 2018. 'Annexin a5 – Chlorambucil: a targeted therapeutic drug against leukemia and breast cancer'*[49].

- Day before starting, autoclave the following items:
  - 1 liter LB medium
  - 4 x 1 liter Erlenmeyer flask (with aluminum foil on top)
  - 125 ml Erlenmeyer flask (with aluminum foil on top)
  - 100 ml beaker (with aluminum foil on top)
  - All size tips
  - 1.5 ml centrifuge tubes (like 100)
  - 1 liter DI water

Protein Expression

Day 1 –9:00 pm

1. Culture 5 µl of *E. coli* BL21(DE3) harboring pET303CT with the fusion gene AV in 10 ml of LB medium containing 35µg/ml kanamycin in a 125 ml Erlenmeyer flask overnight at 37°C with shaking at 200 rpm.
   - LB medium: 1 liter DI H_2O + 10 g Tryptone + 5 g Yeast Extract + 5 g NaCl.
   - Add 35 mg kanamycin to the 1 L of LB medium before taking out the 10 ml for the initial culture.
   - Incubate.

Day 2 - 9:00 am

2. Add 10 ml of the cell culture to 1 liter of fresh culture medium and kanamycin and incubate at 37°C with shaking (200 rpm). Take 1.5 mL of medium before adding the bacteria, as a blank. This cell culture was grown to mid-log phase =>OD_{600} = 0.5.
   - Take a 1.5 ml sample of just the LB medium. Label 1.5 ml tube '**LB**.'
   - Transfer 10 mL of bacteria to 1 L LB medium.
   - Transfer entire volume of medium to 4 x 1 L flasks.
   - Put in shaker at 37° C at 200 rpm.
   - After 1.5 hours of shaking, measure optical density at 600 nm (absorbance) using a clear 96 well plate and microtiter plate reader of sample vs LB medium => using 250 µl samples of each. When OD_{600nm} = 0.5, then proceed to the next step.

Day 2 –2:45 pm

3. Addisopropyl Alpha-D-thiogalactopyranoside to a final concentration of 0.4 mM to solutions in 4 x 1 L flasks and incubate at 30°C with shaking (180 rpm) for 5 h to induce protein expression.
   - Take 750 ml sample of solution before adding IPTG.
   - Add 24 mg IPTG to each flask.
   - Put back in shaker at 30°C for 5 hours.
   - IPTG stimulates the production of fusion protein.

Day 2 – 7:45 pm

4. Harvest the cells by centrifugation for 10 min at 1000 x *g*, at 4ºC.
   - Take 750 ml sample before centrifuge.
   - Centrifuge at 1000xg = 3000 rpm
   - Only 4 – 50 ml centrifuge tubes at a time, temp 4ºC, 10 mins.
   - After first centrifuge, pour out supernatant, add more culture to same 4 tubes. Bacteria will be stuck to side of tubes so inverting to pour out is not a problem.
   - Can put the 4 tubes in -20ºC freezer for overnight storage.

Day 3 – 10 am

5. Resuspend the cell pellet in 40 ml of sonication buffer.
   - Add ~10 ml to each of the 4 centrifuge tubes.
   - Vortex to resuspend cell pellets.
   - Pour contents of the 4 tubes back into the 100 ml beaker.
   - Sonication Buffer
     - 0.05 mM N- *p*-tosyl-L-phenylalanine chloromethyl ketone (TPCK)
     - 1 mM phenylmethylsulfonyl fluoride (PMSF)
     - 1% HPLC ethanol
     - 0.01% βmercaptoethanol
     - 0.02 M sodium phosphate dibasic
     - 40 mL DI
     - Dissolve TPCK and PMSF in ethanol in microcentrifuge tube, then add to beaker.
     - Make this buffer in the 100 ml beaker.
     - Correct to pH 7.4

6. Lyse the cells by sonication at 4ºC for 30 sec at 4.5 watts then allow it to cool for 30 sec on ice. This cycle was repeated 4 times for a total sonication time of 2.5 min on power level 4.
   - Clean sonicator tip with ethanol before use.
   - Put beaker in tub with ice while sonicating.

7. Centrifuge the lysate obtained at 12,000 x *g* for 30 min to remove the cell debris and take the supernatant.
   - Pour beaker contents into 1 purple VWR 50 ml centrifuge tube.
   - Centrifuge at 12000xg for 30 mins
   - Take 750 µl sample after centrifuging.

Protein Purification

Day 3 – 12 pm

8. After taking supernatant sample, add Imidazole (40 mM) and NaCl (500 mM) to the lysate to reduce non-specific protein binding.
   - 40 mM imidazole
   - 500 mMNaCl

9. Equilibrate a 5 ml HisTrap chromatography column with immobilized Ni^{+2}using Wash Buffer 1.
   - Feed wash buffer thru column until the output reaches baseline, then feed lysate thru at -8.00
   - Turn on detector.
   - Turn on drop former – mode 0, rack 1, size 2, last tube 100, min 4, delay 0.
   - WASH BUFFER 1 (500 mL) (- 30 min)
     - 20 mMsodium phosphate dibasic
     - 40 mM imidazole
     - 500 mMNaCl
     - Correct this to pH 7.4

10. Feed the soluble protein fraction into the column.

11. Wash the column with 70 column volumes of Wash Buffer 2 to remove unwanted proteins and endotoxin (250 ml).
   - Collect flow thru – contains unwanted proteins '
   - WASH BUFFER 2 (300 mL) (- 1.5 hours)
     - 20 mM sodium phosphate dibasic
     - 40 mM imidazole
     - 500 mMNaCl
     - 0.1% Trition X-114
     - Correct this to pH 7.4

12. Wash the column with 20 column volumes of Wash Buffer 1 to wash the protein until the pen reaches the baseline (100 ml). (- 40 min)
   - Collect flow thru – contains unwanted proteins

13. Elute the protein using elution buffer.
   - Collect the elution – contains our FP
   - ELUTION BUFFER (300 mL)
     - 20 mM sodium phosphate dibasic
     - 500 mMimidazole
     - 500 mMNaCl
     - Correct this to pH 7

14. Dialyze eluted protein for 3 hours against 2 liters of dialysis buffer containing 20 mM sodium phosphate at pH 7.4 to remove NaCl and imidazole from the protein solution and make it suitable for C-terminal His-tag cleavage.
   - DIALYSIS 1 BUFFER (2 L)
     - 20 mMsodium phosphate dibasic
     - Adjust to pH 7.4
   - After dialysis, put back in a 50 ml centrifuge tube.

15. Before continuing, need to regenerate the column using this procedure:
   - 25 ml of 1 M KCl
   - 25 ml of 1 M NaOH

- 25 ml of DI Water
- 25 ml of 1 M HPLC Grade Ethanol

16. Measure the concentration of protein (Bradford Protein assay).
    - Add 30 ml DI Water to tube with cell pellet.

17. Cleave the C-terminal His-tag by adding HRV 3C protease at 10 U/mg of protein with the recommended 10 X buffer provided. Incubate for 16 h at 4°C at 30 rpm.
    - Add HRV 3C protease. HRV 3C protease comes as 2 U/µl and we want to use it at 10 U/mg protein.

Day 4 – 10 am

18. Equilibrate the HisTrap column with Wash Buffer 1.
    - Feed thru the column until baseline is reached.

Add imidazole (40 mM) and NaCl (500 mM) to the cleaved protein solution (depends on particular volume after overnight cleavage incubation).
- 40 mM imidazole
- 500 mMNaCl

20. Feed the solution to the HisTrap column.
    - Collect first peak solution from the column is solution to dialyze. This contains our protein.

21. Feed Wash Buffer 1 into column to pull out all cleaved protein before proceeding forward.

22. Elute uncleaved protein with imidazole.

23. Dialyze purified protein for 3 hours against 2 liters of dialysis buffer.
    - DIALYSIS 2 BUFFER
      - 20 mM sodium phosphate dibasic
      - 100 mMNaCl
      - Adjust to pH 7.4

24. Regenerate the column as above.

25. Pass the sample thru a 0.2 µm cellulose-acetate filter.

26. (IF NECESSARY) Concentrate the protein using a 150 kDa, 20 ml protein concentrator (Millipore #89921).

27. Aliquot purified protein into cryovials and put in the liquid nitrogen tank prior to freeze-drying.

30. Perform an SDS-PAGE
    - Suspend 50 µl of sample + 50 µl loading buffer (95% Laemmli sample buffer + 5% β-mercaptoethanol).
    - For BI, centrifuge for resuspend in 100 µl of loading buffer.

Appendix B: SWCNT-annexin V conjugation protocol

Protocol from Dr. Patrick McKernan, source: *McKernan, Patrick. 2018. 'Therapeutic Applications of Bioconjugates in Human Disease'* [38].

1. Prepare 1% SDS solution.
    a. Prepare 1% SDS stock.
        i. .5g SDS in 50mL DI water.
2. Prepare SWCNT suspensions.(2 hours and 45 minutes→store in the fridge)
    a. Sonicate the SWCNT solution for 30 minutes. (6mg SWCNT in 5 ml 1% SDS)
        a. Use SG65i from 5/13/2013.
    b. Make solution in a glass vial.
    c. Sonicate a maximum. (difficulty turning on/make sure probe does not touch the glass vial)
    d. Place vial in water bath to prevent it from overheating.
    b. Centrifuge the SWCNT solution for 30min at 13000rpm.
        a. Store supernatant.
        b. Aggregates will drop to the bottom of solution.
    c. Transfer SWCNTs supernatant solution to new tube and repeat steps a and b.
3. Dissolve DSPE-PEG-Maleimide linker (MW 4368 Da) at 1.5 mg/ml in 1% SDS.
    a. Dissolve 1.5mg of linker in 1mL 1% SDS.
    b. Store linker at -20˚C under nitrogen.
4. Add 1 ml of linker to 5 ml of SWCNT suspension.
5. Mix at RT for 30 min with gentle shaking on shaker with stir bar.
6. Dialyze SWCNT-linker for 8 hr against 2 L of DI water. Change the dialysate after 4 hr. Use a 2 kD dialysis membrane.
    a. Use green dialysis clips.
7. Reconstitute 5 mg of annexin a protein with 1 ml of DI water.
    a. Conduct a Bradford Assay to confirm protein concentration.
        i. Mix 5uL of protein and 250uL of Bradford reagent in 96-well plate with clear bottom. Run blank well with DI water. (use aliquot)

ii. Shake for 30 seconds and incubate at room temperature for 10 minutes.
iii. Read absorbance at 595nm. Absorbance should be between 0.3-1.
iv. Use standard curve equation to determine concentration.

8. Take 2 ml of SWCNT-linker suspension and add 5mg of annexin A5 to it. (annexin:linker molar ratio= 1.05:1)
9. Mix the SWCNT-linker and annexin A5 at RT for 2 hr with gentle shaking on shaker (3 ml total volume).
10. Block unreacted linker sites with 0.166 mg of L-cysteine and mix at RT for 1 hr with gentle shaking. (The molar ration of L-cys:linker is 4:1) For ease, add 33.2µl of a 5 mg/ml solution of L-Cysteine.
11. Dialyze the SWCNT-annexin A5 conjugate for 8 hr against 2 L of 20 mM sodium phosphate buffer at pH 7.4 (5.678 g of sodium phosphate/2L DI water). Change the dialysate after 4 hr. Use a 100kD dialysis membrane. Do not allow this dialysis to go to long—change the dialysate at 3:45 and remove from dialysis at 7:30.
12. Centrifuge the resulting SWCNT-annexin A5 conjugate at 15,680g for 1 hr to remove aggregates.
    a. Keep supernatant.
13. Measure the SWCNT and protein concentrations.
    a. Run Bradford assay for protein concentration.
    b. Measure SWCNT absorbance at 800nm of spec.
14. Store conjugate at 4˚C.

Appendix C: Cytokines standard curves

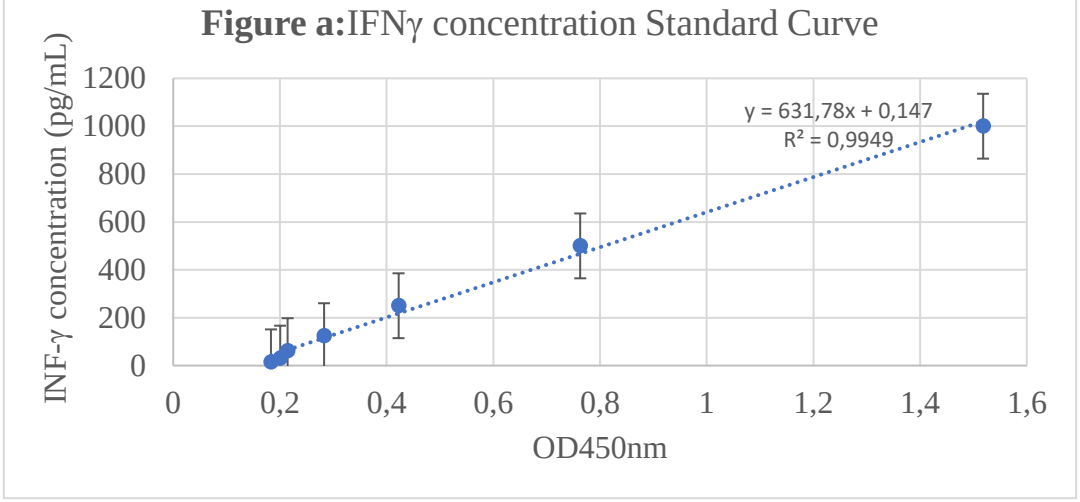

Figure a: IFNγ concentration Standard Curve

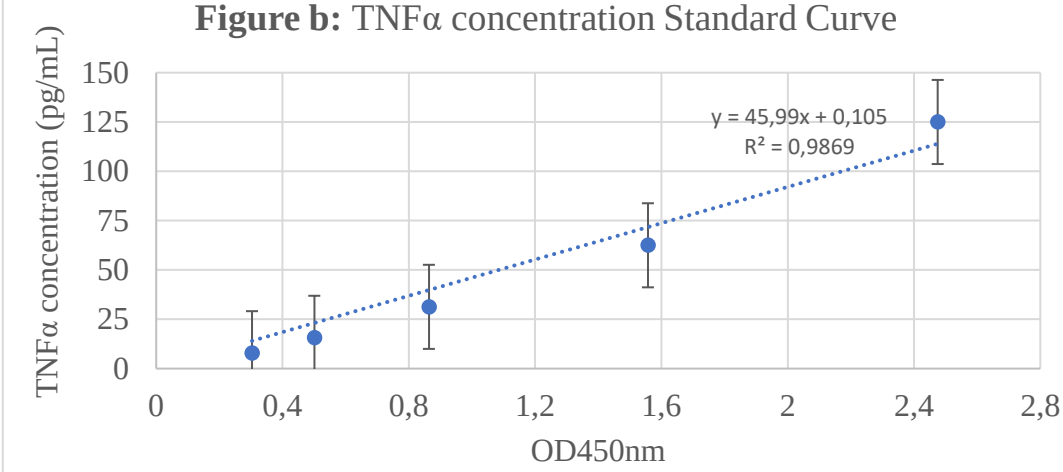

Figure b: TNFα concentration Standard Curve

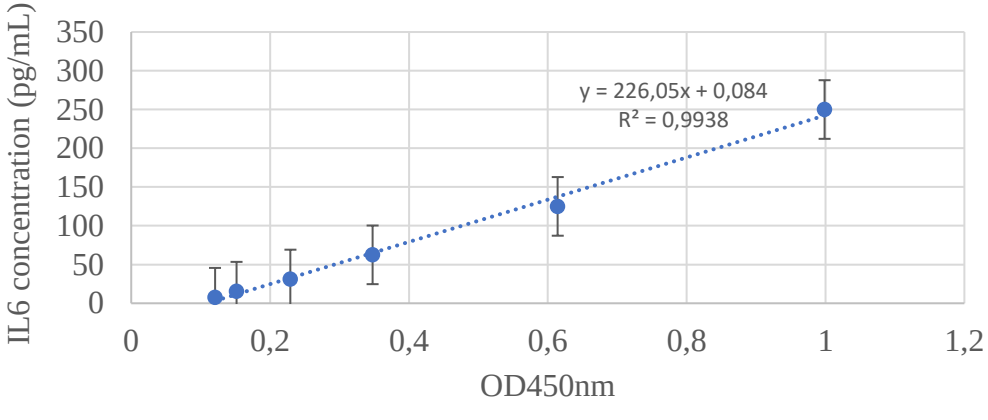

Figure c: IL6 concentration Standard Curve